Orientation Effects on Nitric Acid Dihydrate Films

ARTICLE *in* THE JOURNAL OF PHYSICAL CHEMISTRY B · MAY 2006

Impact Factor: 3.3 · DOI: 10.1021/jp0569483 · Source: PubMed

5 AUTHORS, INCLUDING:

Belén Maté
Spanish National Research Council
76 PUBLICATIONS **829** CITATIONS
SEE PROFILE

Ismael K. Ortega
The French Aeropace Lab ONERA
64 PUBLICATIONS **805** CITATIONS
SEE PROFILE

Miguel Angel Moreno Alba
Spanish National Research Council
28 PUBLICATIONS **243** CITATIONS
SEE PROFILE

Orientation Effects on Nitric Acid Dihydrate Films

Belén Maté,* Ismael K. Ortega,† Miguel A. Moreno, Victor J. Herrero, and Rafael Escribano

Instituto de Estructura de la Materia (CSIC), Serrano 123, 28006 Madrid, Spain

Received: November 30, 2005; In Final Form: February 9, 2006

An investigation of orientation effects in films of nitric acid dihydrate (NAD) is presented, based on a systematic study of transmission and reflection−absorption infrared (RAIR) spectra of samples of varying thickness. The samples are prepared by vapor deposition on Ge (for transmission spectroscopy) and on Al substrates (for RAIR spectroscopy) at 175 K to produce crystalline α-NAD films. Transmission spectra were recorded at normal incidence, and RAIR spectra were recorded at a grazing angle of 75°, with polarized radiation. The observed spectra are compared with predictions of a classical Fresnel model, to test the available optical indices of NAD, which are of great importance for the accurate interpretation of data from remote sensing measurements. Whereas the procedure yields satisfactory results for transmission and s-polarized RAIR spectra, it is found that the agreement is not acceptable for p-polarized RAIR spectra. An explanation is suggested in terms of a preferential alignment of the films, with the (10−1) crystallographic plane of the crystal situated parallel to the substrate. The infrared activity of a band at ≈1170 cm^{-1} is explained in terms of a preferential orientation of the crystal domains in the film.

1. Introduction

The equilibrium phase diagram of the system HNO_3/H_2O has been studied carefully by Grothe and collaborators[1] and contains two thermodynamically stable hydrates, the monohydrate (NAM) and the trihydrate (NAT). NAT has received considerable attention as the most likely candidate for type Ia polar stratospheric clouds (PSC), due to its thermodynamic stability under polar stratospheric conditions. But some works suggest that nitric acid dihydrate (NAD),[2−4] a metastable phase, can also form and persist in the winter stratosphere, since the formation of a given species in that region is often not controlled by thermodynamics but by kinetics. Two crystal structures of NAD were determined by Lebrun et al.[5,6] The low-temperature phase, NAD(I) or α-NAD, is monoclinic. It has a layer structure, the layers being bound by weak van der Waals forces and weak hydrogen bonds. In the crystal all nitric structures are ionic (NO_3^-) and the water units appear as either $H_5O_2^+$, H_3O^+, or H_2O, linked by hydrogen bonds. The high-temperature phase, NAD(II) or β-NAD, has similar molecular composition and distribution, but the cell parameters are quite different.

One of the most common techniques used for the phase characterization and for thermodynamic and kinetic studies of phase transitions and chemical reactions involving nitric acid hydrates is infrared (IR) spectroscopy. Most of the IR spectroscopic studies of crystalline NAD were made before the discovery of the α and β varieties. At that time the crystals were termed just NAD, but the phase studied was always the low-temperature phase α-NAD. As far as we know, there is only one publication, by Grothe et al.,[7] where a spectrum of the high-temperature phase β-NAD is presented.

Transmission IR spectra attributed to crystalline α-NAD films have been published by several groups.[8−10] These crystalline α-NAD films were obtained in different ways. Ritzhaupt et al.[8] deposited H_2O and HNO_3 vapor on a substrate at 80 K and then annealed it to the crystalline form at 175 K. Koehler et al.[9] deposited the vapors directly on a substrate at 183 K. Koehler et al. also carried out thermal programmed desorption measurements with mass spectrometric detection of the products to provide a link between the stoichiometry of the deposited samples and the IR spectra. The spectra obtained in both laboratories were similar. Transmission IR spectra were first assigned on the basis of available spectroscopic information on the individual molecules and ions present in the α-NAD structure.[8,11] Only recently, Fernandez et al.[12] were able to assign the spectra of several nitric acid hydrates, and in particular of α-NAD, using first principle calculations. They found a good overall agreement between experiment and calculated spectra. Also, Toon el al.[10] determined frequency-dependent complex refractive indices for crystalline α-NAD from IR transmission spectra of films of different thickness. These optical constants are necessary for the identification of these species in the stratosphere.[13,14]

Laboratory-generated α-NAD aerosols have also been studied by IR spectroscopy.[3,4,15−17] These experiments reproduced more closely the PSC morphology and the conditions of the stratosphere. The extinction spectra obtained showed an overall reasonable agreement with results from thin film experiments, although some significant differences were found in the intensities of several absorption bands, especially in those below 1500 cm^{-1}. Niedziela et al.[16] determined the IR complex refractive indices of crystalline α-NAD between 700 and 4700 cm^{-1} from aerosol extinction spectra using a Mie scattering model.

The work of Tisdale et al.[18] presented a careful study of the variation of the IR transmission spectra of α-NAD films with formation conditions. They found only minor variations between spectra of films grown at different temperatures. However, major differences were observed between the spectra of annealed films, vapor deposited films, and particles. They concluded that the differences observed were mainly due to compositional effects, although formation temperature, formation method, or the

* Corresponding author. E-mail: bmate@iem.cfmac.csic.es.

† Also at Departamento de Química Física y Analítica, Universidad de Jaén, Paraje Las Lagunillas, 23071 Jaén, Spain.

10.1021/jp0569483 CCC: $33.50
Published on Web 03/21/2006

substrate could also have an influence. They studied also α-NAT films, and in that case crystal orientation in the films was mentioned as another possible explanation for the variations observed in the spectra.

RAIR spectra of crystalline NAD films were also recorded in different laboratories.[7,11,19,20] Several differences in band intensities were observed between RAIR and transmission spectra. They were attributed, in principle, to optical effects, purity of the samples, and/or degree of crystallinity. However, we found clear evidences of orientation effects in α-NAT films. Our study was based on polarized RAIR spectroscopy and reported in a recent publication.[21] An evidence was the polarization-dependent behavior of the IR band observed at 1140 cm^{-1}.

In the present work, motivated by our findings in crystalline α-NAT films,[21] we have carried out a systematic study of crystalline α-NAD films, looking for similar orientation evidences. We have recorded transmission and grazing angle RAIR polarized and nonpolarized spectra of crystalline α-NAD films of different thickness. The experimental measurements are compared with Fresnel model simulations for RAIR and for transmission spectra, using the method described in refs 22 and 23. The spectral features are discussed using the previously reported theoretical assignments of the spectrum of the crystal.[12]

2. Experimental Section

Nitric acid dihydrate films were grown and studied with RAIR and transmission spectroscopy using the experimental setup described in detail elsewhere.[24] Briefly, ice films were generated on a ultrahigh vacuum cylindrical chamber, evacuated by a turbomolecular pump and provided with a liquid nitrogen Dewar in contact with the deposition substrate. After filling the Dewar, the base pressure was in the 10^{-9} mbar range. The cold deposition surface used for RAIR experiments was made of polished aluminum, and the surface temperature could be regulated between 85 and 323 K with an accuracy of 1 K. For transmission experiments we have used an IR transparent germanium substrate 2 mm thick. It has been mounted on a new holder that allows the control of the substrate temperature between 90 and 320 K with an estimated accuracy of 1 K. The temperature control is carried out in a similar way as in the RAIR experiment. Two independent inlets, for water and nitric acid, were used to introduce the vapors and backfill the chamber. The purity of the species introduced into the chamber was measured with a quadrupole mass spectrometer.

To obtain α-NAD films we followed the phase diagram obtained for the H_2O:HNO_3 system by Tizek et al.[1] The deposition surface (Al or Ge) was maintained at 175 K, and the chamber was filled with a controlled amount of H_2O and HNO_3. The H_2O:HNO_3 ratio was selected to be greater than the stoichiometric 2:1 value in order to obtain α-NAD.[1] The total pressure in the chamber was around 7×10^{-5} mbar. It was stable during all the deposition time but slightly different for experiments carried out in different days. Similar experimental conditions have been used to grow the α-NAD films for the transmission and RAIR experiments.

In the RAIR experiment the film thickness could be approximately measured (with an estimated uncertainty of ±10%) by monitoring the interference fringes of a He−Ne laser incident on the growing film at near normal incidence. With this technique we estimated a growing speed of 30 nm/min.

To stabilize the α-NAD film in order to record the s-polarized, p-polarized, and the nonpolarized RAIR spectra, the substrate temperature was lowered to 155 K, after removing the gas phase.

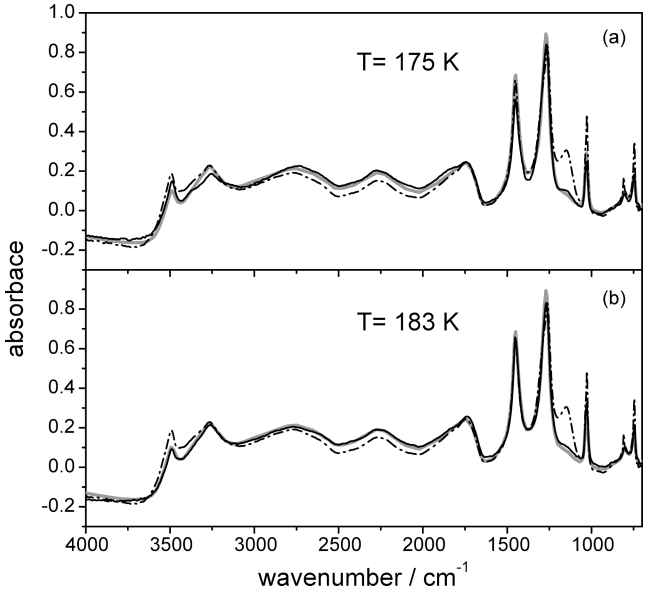

Figure 1. Transmission spectra of α-NAD films (solid line, experimental) compared with Fresnel simulations carried out with the optical indices of Toon et al.[10] (gray line) and Niedziela et al.[16] (dash−dotted line). Film thickness determined from simulation: $d = 600$ nm at each side of the Ge substrate. Panel a shows the film grown at 175 K, 30 nm/min and panel b the film grown at 183 K, 100 nm/min.

For the faster transmission spectra, a small thickness variation during the measurements is not relevant, and all the spectra were taken at 175 K.

To accurately simulate the conditions used in the experiment of Toon et al.,[10] for some transmission experiments the films were generated using different growing conditions: The substrate was kept at 183 K and the total pressure in the chamber was 2×10^{-4} mbar, giving a growing speed of approximately 100 nm/min.

A Brucker IFS66 FTIR spectrometer was used to record the spectra. The IR radiation was focused on the sample with a KBr lens at an incidence angle of 75° for RAIR configuration and at normal incidence for the transmission setup. The reflected, or transmitted, IR light was focused on a MCT detector cooled with liquid nitrogen. In the RAIR configuration, a polarizer (SPECAC KRS-5), placed before the focusing lens, was used to select the polarization of the incident radiation. With the electric field vector perpendicular or parallel to the incidence plane, we recorded the corresponding s- or p-polarized spectra. Each spectrum was obtained from the addition of 512 scans recorded at 8 cm^{-1} apodized resolution.

3. Results

3.1. Transmission Spectra. In Figure 1a we present an example of a transmission spectrum of a crystalline α-NAD film obtained from vapor deposition at 175 K on both sides of a Ge substrate. The experimental spectrum is compared with spectral simulations carried out using the method described in ref 23 for a three layer system, considering normal incidence and total coherence. The imaginary part of the Ge refractive index has been neglected, and for the real part a constant value of $n = 4$ has been taken in all the frequency range of our experiment.[25] The optical constants for crystalline α-NAD were taken from the two sets of values available in the literature: that by Toon et al.,[10] obtained from thin film transmission spectra at 184 K, and the set determined by Niedziela et al.,[16] from aerosol extinction spectra at 180 K. The agreement between experiment and simulation for the indices of Toon et

al. is very good, but it is not so good for the aerosols indices of Niedziela et al. The film thickness determined from the simulation is $d = 600$ nm on each side of the substrate. The simulation with the thin film indices is in very good agreement with the measurements, and only very slight differences are observed in the 3250−3500 cm^{-1} region and in the 1450 cm^{-1} peak. In contrast, the simulation with the aerosols indices overestimates the region above 3000 cm^{-1} and underestimates the region between 1700 and 3000 cm^{-1}. The feature at 1170 cm^{-1}, absent from the optical indices of Toon et al. but present in those of Niedziela et al., appears as a very small shoulder in our transmission spectra, in better agreement with the indices of Toon et al. We can conclude that the crystalline α-NAD films obtained in our laboratory on Ge at 175 K are very similar to those grown by Toon et al. on a silicon substrate at 184 K. Considering the phase diagram of Tizek et al.,[1] both temperatures, 175 and 184 K, could give crystalline α-NAD if the H_2O:HNO_3 ratio is adequate.

Another comparison between experimental and simulated transmission spectra is presented in panel b of Figure 1. We simulated in our lab the growing conditions of Toon et al. and deposited the vapors on a substrate at 183 K, with a total pressure that gave a growing speed of 100 nm/min (similar to the one used by Toon et al.[10]). In this case the agreement between experiment and simulation with the thin film indices is almost perfect. The effect of using different substrates seems imperceptible. However, the simulation with the aerosol indices shows again noticeable differences.

These experiments were meant to show the differences caused in the films, and evidenced in the spectra, by different growing conditions. In both cases, parts a and b of Figure 1, the agreement between the experimental spectra and the simulations with the indices of Toon et al. is good, but a close inspection reveals small differences in the α-NAD spectra recorded at the two temperatures. The band that provides a strong evidence of α-NAD film orientation, as we will discuss below, is the one at 1170 cm^{-1}, and we want to emphasize that it is lacking in the two experimental spectra presented in Figure 1.

3.2. RAIR Spectra. In Figures 2, 3, and 4 we present the nonpolarized and p- and s- polarized RAIR spectra obtained for α-NAD films of thickness 400, 580, and 710 nm, respectively. The growing conditions were the same as those used to obtain the film for the transmission spectrum in Figure 1a, with the substrate at 175 K. Before starting to record the spectra the films were stabilized by cooling to 155 K. The RAIR experimental spectra are compared with simulations carried out with the indices of Toon et al.[10] and Niedziela et al.[16] using a Fresnel model.[22]

In the s-polarization the electric field is perpendicular to the incident plane, which implies that it is contained in the plane of the substrate. The metal surface selection rule (MSSR) in grazing angle RAIR spectroscopy nearly cancels the electric field at the surface of the metal,[26] and for that reason, the s-polarized spectra is nonexistent for very thin films (approximately for $d < 100$ nm). For films several hundred nanometers thick, the MSSR relaxes and some s-polarized spectra emerge.

For the p-polarization, the electric field is contained in the plane of incidence. Due to the MSSR at the metal surface, the electric field is perpendicular to the substrate. Also, it gives rise to an intensity enhancement of the electric field in that direction. When the MSSR relaxes, the electric field is no longer strictly perpendicular to the substrate surface, and the intensity enhancement is smaller. Figure 2 corresponds to a film of $d =$ 400 nm where the MSSR is partially relaxed and the s-polarized spectrum (Figure 2c) is visible (but with a poor signal-to-noise ratio), while the p-polarized spectra (Figure 2b) is intense due to the intensity enhancement caused by the MSSR.

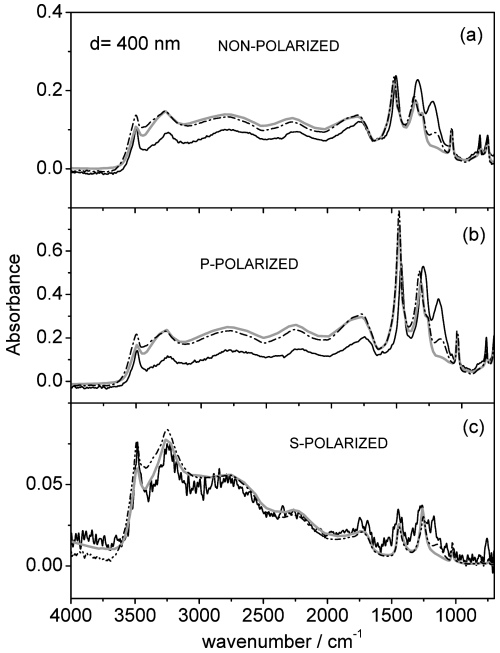

Figure 2. Grazing angle RAIRS spectra of an α-NAD film grown at 175 K, with $d = 400$ nm. The experimental spectra are given by solid lines; simulations with the indices of Toon et al.[10] and Niedziela et al.[16] are shown with gray and dash−dotted lines, respectively: (a) nonpolarized, (b) p-polarized, (c) s-polarized spectra.

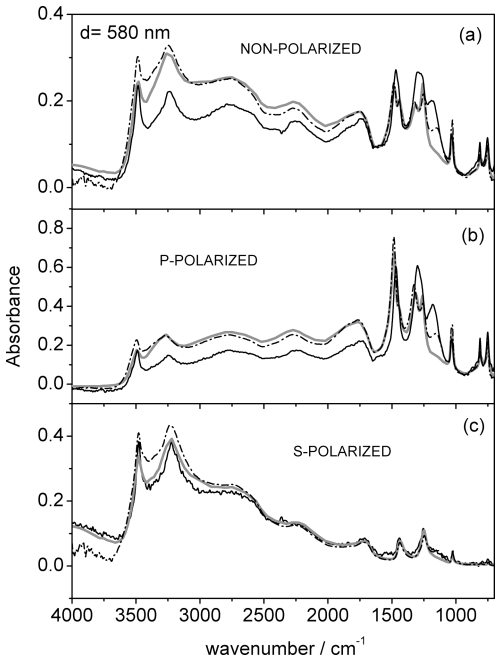

Figure 3. Same as in Figure 2 but corresponding to a film with $d =$ 580 nm.

In the s-polarized spectra presented in Figures 2c−4c, a very good agreement is found between the simulations made with the optical indices of Toon et al. and the experimental spectra. As mentioned in the Experimental Section, we are able to estimate the film thickness from the interferences of a He−Ne laser. In RAIR experiments, we needed to stabilize the film in order to record s-, p-, and nonpolarized spectra of a film of a given thickness. For this purpose, we chose to remove the gas

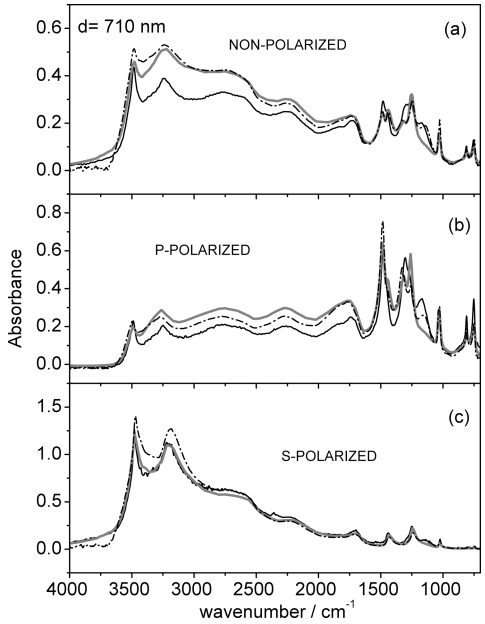

Figure 4. Same as in Figure 2 but corresponding to a film with $d =$ 710 nm.

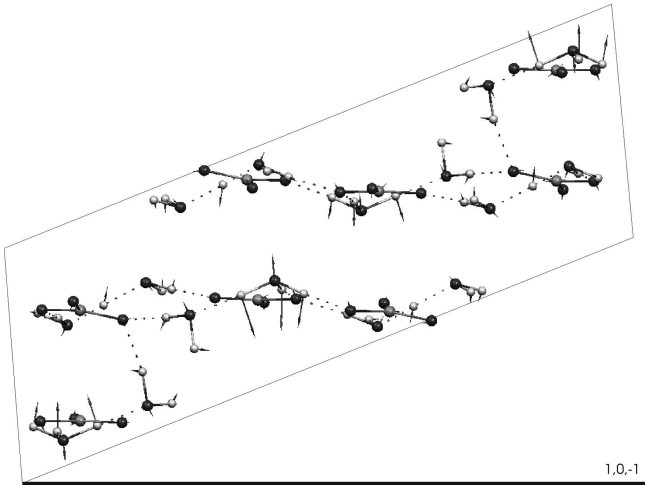

Figure 5. Unit cell of α-NAD containing the "$a-c$" plane, with the cell axis "b" perpendicular to the page. Arrows indicate the atom displacements in the 1181 cm^{-1} normal mode calculated by Fernández et al.[12] The horizontal line is the intersection of the (10−1) crystallographic plane with the surface of the paper.

phase, to prevent further growing, and then to cool the film to 155 K. Part of the film was desorbed during this process. The accuracy of the thickness measurement was lost due to the impossibility of measuring precisely the amount of film desorbed. However, the He−Ne measurement allows a first estimate. The final film thickness given in Figures 2−4 has been determined as that which gives the best fit of the simulated s-polarized spectra with the experiment. Comparing the film thickness measured from the interference technique with the values obtained from the simulation, we found that the latter are roughly 20% smaller.

It should be mentioned that the s-polarized spectrum in Figure 4 becomes very intense (even more intense than the corresponding p-polarized spectrum) in the 3000 cm^{-1} frequency range, due to an infrared interference. IR interferences are an optical effect that appears in RAIR spectroscopy and have been explained in more detail elsewhere.[22] In essence, the increase in intensity is not due to an absorption of the ice film but to a destructive interference of the IR radiation that occurs for a particular film thickness at a particular frequency. In the case of Figure 5 the IR intereference appears at around 3000 cm^{-1} for a film thickness of 710 nm. The IR interferences are taken into account in the Fresnel model and reproduced properly by the indices of Toon et al.

s-Polarized spectra are clearly worse reproduced by the simulation with the aerosol indices of Niedziela et al., where the high-frequency region of the spectra, between 3000 and 3700 cm^{-1}, is overestimated by the simulation.

The simulations of the p-polarized spectra (see Figures 2b−4b) systematically overestimate the absorption in the frequency range from 3600 to 1500 cm^{-1}. The experimental peak at 1480 cm^{-1} is also overestimated and, on the contrary, the band at 1300 cm^{-1} is underestimated. For the thinnest film studied, with $d =$ 400 nm (Figure 2b), two unresolved peaks at 1320 and 1270 cm^{-1} appear in the simulation with the indices of Toon et al. under the experimental band at 1300 cm^{-1}. With increasing film thickness (Figures 3b and 4b), the low-frequency simulated peak at 1270 cm^{-1} increases in intensity and distorts the simulated spectrum. This effect does not appear so evident in the aerosol indices simulations. In addition, the experimental band observed at 1170 cm^{-1} in all the p-polarized spectra is missing in all the simulations with the indices of Toon et al. and is present, although relatively weak, in the aerosol indices simulations. Note that in the low-frequency region between 1300 and 1100 cm^{-1} the aerosol indices of Niedziela et al.[16] reproduce better the experimental p-polarized RAIR spectra than the indices of Toon et al.[10]

The nonpolarized spectra presented in Figures 2a−4a are an average of the corresponding s- and p-polarized spectra of each film, and consequently, the simulations do not match the measured data.

4. Discussion

4.1. Comparison of Experiment vs Simulation. It is worth observing in Figures 2−4 the good agreement found between the spectra simulated with the indices of Toon et al.[10] and our experimental spectra for s-polarization, in contrast with the poor agreement found for p-polarized and nonpolarized spectra. However, the p-polarized spectra are better simulated with the indices of Niedziela et al.[16] In the s-polarized spectra, the electric field is contained on the substrate plane while in the p-polarized spectra the electric field is almost perpendicular to that plane. Taking into account that the technique used by Toon and coworkers[10] was normal incidence transmission spectroscopy, for which the electric field is contained in the plane of the substrate, it seems logical that their data can reproduce better the s-polarized spectra. The fact that the p-polarized and nonpolarized spectra are not well reproduced with the indices of Toon et al. indicate that maybe the α-NAD films are not isotropic and the optical constants of Toon et al. describe only the crystal in the plane of the substrate, but a different set of optical constants may be needed to describe these films in the direction perpendicular to the substrate. The above observations indicate that the polycrystalline α-NAD film is oriented and that there is a preferential alignment of the crystal domains in the growing process.

The aerosol indices of Niedziela et al. for α-NAD are obtained by applying Mie scattering theory.[16] Those indices simulate properly neither transmission nor RAIR spectra of α-NAD films, as has been shown in Figures 1−4. This behavior supports our interpretation of the orientation of the α-NAD films as anisotropic films that cannot be simulated properly with indices that

TABLE 1: Calculated Wavenumbers for the Normal Modes of Crystalline α-NAD and Proposed Assignment to the Predominant Molecular Vibrations (reproduced from Table 2 of ref 12)

wavenumber range[a]	predominant vibrations[b]
3489−3470 (4)	$\nu_3(H_2O)$ a-s
3333−3297 (4)	$\nu_3(H_2O)$ a-s + $\nu_3(H_3O^+)$ a-s
3179−3136 (8)	$\nu_3(H_2O)$ a-s + $\nu_3(H_3O^+)$ + $\nu_1(H_3O^+)$
3017−2982 (4)	$\nu_1(H_3O^+)$ s-s + $\nu_3(H_3O^+)$ a-s
2946−2907 (4)	$\nu_3(H_3O^+)$ a-s
2801−2763 (4)	$\nu_1(H_3O^+)$ s-s
2610−2454 (8)	$\nu_3(H_3O^+)$ a-s
1793−1642 (20)	$\nu_4(H_3O^+)$ a-b
1574−1435 (16)	$\nu_3(NO_3^-)$a-s + $\nu_2(H_2O)$b + $\nu(H_5O_2^+)$ s
1339−1303 (8)	$\nu_3(NO_3^-)$ a-s + $\nu_2(H_3O^+)$ s-b
1295−1263 (4)	$\nu_2(H_3O^+)$ s-b + $\nu_3(NO_3^-)$ a-s
1213−1181 (4)	$\nu_2(H_3O^+)$ s-b
1054−1043 (8)	$\nu_1(NO_3^-)$ s-s

[a] Number in parentheses indicates number of fundamental modes grouped in this range. [b] s-, symmetric; a-, asymmetric; s, stretching; b, bending.

assume the sample to be isotropic. In this interpretation two set of indices would be required for a correct description of a nonisotropic crystal, one for the optical properties within the plane of the substrate and the other for the plane perpendicular to the substrate. The indices of Toon et al. correspond to the former and therefore give a good interpretation of s-polarized spectra. On the other hand, those of Niedziela et al., determined from aerosol particles, represent an average of the two sets and do not provide an accurate representation in any case but afford a better interpretation of the p-polarized spectra than those of Toon el al., because of the contribution of information from the perpendicular plane.

4.2. Vibrational Analysis. We present in this paragraph an interpretation of the effects mentioned above, based on an analysis of the vibrational modes of the crystal reported in a previous work.[12] In this interpretation we have been mainly guided by the strong sensitivity to orientation found in the experimental band of α-NAD at 1170 cm^{-1}. This band is almost missing in transmission and s-polarized spectra. However, it appears with higher or lower intensity in all the RAIR spectra of α-NAD found in the literature. It is a quite intense band in the p-polarized spectra presented in this work, as can be seen in Figures 2b−4b. The behavior of this band suggests that it is associated with a crystal mode giving rise to a dipole moment almost perpendicular to the substrate plane. In the calculated wavenumber list for normal modes of crystalline α-NAD given in Table 2 of our previous work,[12] reproduced partially in Table 1 here, the mode at 1181 cm^{-1} and those close to it at slightly higher frequencies are the nearest to the experimental band at 1170 cm^{-1}. These modes are assigned to the experimental band under discussion. The corresponding atomic displacements were associated with the H_3O^+ symmetric bending.[12] In Figure 5, the movements of the atoms in the normal mode at 1181 cm^{-1} are represented with arrows. The horizontal plane normal to the surface of the paper represents the crystallographic plane (10−1), and it corresponds to the molecular layer present in the α-NAD structure. The symmetric bending of the H_3O^+, which takes place in a direction perpendicular to this plane, generates a dipole moment mostly perpendicular to it. If the plane (10−1) were parallel to the substrate in the growing α-NAD film, this would explain the observations of polarized RAIR spectroscopy with respect to the 1170 cm^{-1} band.

In a similar way, but with unnoticeable effects on the spectrum, the symmetric stretching of H_3O^+, having the same symmetry as the bending, would induce a dipole moment change oriented perpendicularly to the substrate plane. The symmetric and asymmetric stretchings are heavily mixed (see Table 1), appearing as a broad feature in the 2500−3000 cm^{-1} region, where no conclusive changes are observed in the experimental s- and p-RAIR spectra.

This interpretation is consistent with the rest of the assignments. Most crystal modes generate dipole moments with components parallel and perpendicular to the (10−1) plane.

5. Summary and Conclusions

We present in this work transmission and grazing angle RAIR p-polarized, s-polarized, and nonpolarized spectra of α-NAD films formed by vapor deposition at 175 K. RAIR spectra were recorded for films of thicknesses between 400 and 710 nm. The comparison of the transmission and RAIR spectra with simulations carried out with Fresnel models and the optical indices from the literature has revealed evidence of anisotropy in the α-NAD films studied. The s-polarized spectra were very well simulated with the optical indices of Toon et al.,[10] obtained from transmission spectra of α-NAD films. However, the p-polarized spectra could not be reproduced with these indices and, in some regions, were better simulated with the indices of Niedziela et al.,[16] obtained from NAD aerosols. If the direction of the IR electric field in relation with the substrate plane is considered for each spectroscopic technique, it is possible to understand these effects by means of a preferential orientation of the α-NAD crystal domains in the films. A preferential growing of the α-NAD film with the (10−1) crystallographic plane parallel to the metal substrate is the best explanation. This orientation seems independent of the particular substrate used (Al, Si, Ge) and on the growing conditions (at least for those growing conditions used in the present work and in the literature). The (10−1) plane is the one defined by the molecular layers found in the X-ray studies of Lebrun[5,6] in the structure of the α-NAD crystal. The successive layers are bound by weak van der Waal forces, and thus, the adsorption of a layer parallel to the substrate can be energetically favorable, since it does not disrupt a strong crystal structure.

PSC type Ia particles are characterized by strong depolarization in LIDAR observations, which indicate aspherical particle shapes.[27,28] The exact composition of those type Ia PSC particles is still under debate. The presence of nitric acid trihydrate seems to be confirmed,[14,29] but the existence of nitric acid dihydrate has also been postulated.[2,3] The effects of particle shape on band positions and intensities in extinction infrared spectra of NAD aerosols have been studied recently in the laboratory.[17] In this work we have focused on anisotropic effects in NAD crystals. This anisotropy could also be present in the aspherical NAD particles. To extract information about composition and physical properties of those PSC particles from satellite mid-infrared spectra, accurate reference spectra of the various components are necessary. Such reference spectra are based on optical constants that have been determined in the laboratory. The anisotropic effects in NAD crystals should be taken into account to determine precise optical constants that will allow accurate interpretations of satellite retrievals.

Acknowledgment. This investigation has been funded by Project FIS2004-00456 of the Spanish Ministry of Education and carried out within the frame of a "Unidad Asociada" between IEM (CSIC, Madrid) and the Department of Analytical and Physical Chemistry of the University of Jaén.

References and Notes

(1) Tizek, H.; Knözinger, E.; Grothe, H. *Phys. Chem. Chem. Phys.* **2002**, *4*, 5128.

(2) Worsnop, D. R.; Fox, L. E.; Zahniser, M. S.; Wofsy, S. C. *Science* **1993**, *259*, 71.

(3) Disselkamp, R. S.; Anthony, S. E.; Prenni, A. J.; Onasch, T. B.; Tolbert, M. A. *J. Phys. Chem.* **1996**, *100*, 9127.

(4) Bertram A. K.; Sloan, J. J. *J. Geophys. Res.* **1998**, *103* (D3), 3553−3561.

(5) Lebrun, M.; Mahe, F.; Lamiot, J.; Foulon, M.; Petit, J. C.; Prevost, D. *Acta Crystallogr.* **2001**, *B57*, 27.

(6) Lebrun, M.; Mahe, F.; Lamiot, J.; Foulon, M.; Petit, J. C. *Acta Crystallogr.* **2001**, *C57*, 1129.

(7) Grothe, H.; Myhre, C. E. L.; Tizek, H. *Vib. Spectrosc.* **2004**, *34*, 55.

(8) Ritzhaupt, G.; Devlin, J. P. *J. Phys. Chem.* **1991**, *95*, 90.

(9) Koehler, B. G.; Middlebrook, A. M.; Tolbert, M. A. *J. Geophys. Res.* **1992**, *97*, 8065.

(10) Toon, O. B.; Tolbert, M. A.; Koehler, B. G.; Middlebrook, A. M.; Jordan, J. *J. Geophys. Res.* **1994**, *99* (D12), 25631.

(11) Koch, T. G.; Holmes, N. S.; Roddis T. B.; Sodeau, J. R. *J. Chem. Soc., Faraday Trans.* **1996**, *92*, 4787.

(12) Fernández, D.; Botella, V.; Herrero, V. J.; Escribano, R. *J. Phys. Chem. B* **2003**, *107*, 10608.

(13) Herving, M. E.; Deshler, T. *J. Geophys. Res.* **1998**, *103* (D19), 25345.

(14) Höpfner, M.; Luo, B. P.; Massoli, P.; Cairo, F.; Spang, R.; Snels, M.; Di Donfrancesco, G.; Stiller, G.; von Clarmann, T.; Fischer, H.; Biermann, U. *Atmos. Chem. Phys. Discuss.* **2005**, *5*, 10685−10721.

(15) Barton, N.; Rowland, B.; Devlin, J. P. *J. Phys. Chem.* **1993**, *97*, 5848.

(16) Niedziela, R. F.; Miller, R. E.; Worsnop, D. R. *J. Phys. Chem. A* **1998**, *102*, 6477.

(17) Wagner, R.; Möhler, O.; Saathoff, H.; Stetzer, O.; Schurath, U. *J. Phys. Chem. A* **2005**, *109*, 2572.

(18) Tisdale, R. T.; Prenni, A. J.; Iraci, L. T.; Tolbert, M. A.; Toon, O. B. *Geophys. Res. Lett.* **1999**, *26*, 707.

(19) Barone, S. B.; Zondlo, M. A.; Tolbert, M. A. *J. Phys. Chem. A* **1997**, *101*, 8643.

(20) Escribano, R.; Couceiro, M.; Gómez, P. C.; Carrasco, E.; Moreno, M. A.; Herrero, V. J. *J. Phys. Chem. A* **2003**, *107*, 651.

(21) Maté, B.; Ortega, I. K.; Moreno, M. A.; Escribano, R.; Herrero, V. J. *Phys. Chem. Chem. Phys.* **2004**, *6*, 4047.

(22) Maté, B.; Medialdea, A.; Moreno, M. A.; Escribano, R.; Herrero, V. J. *J. Phys. Chem. B* **2003**, *107*, 11098.

(23) Fernández-Torre, D.; Escribano, R.; Herrero, V. J.; Maté, B.; Moreno, M. A.; Ortega, I. K. *J. Phys. Chem. B* **2005**, *109*, 18010.

(24) Carrasco, E.; Castillo, J. M.; Escribano, R.; Herrero, V. J.; Moreno, M. A.; Rodríguez, J. *Rev. Sci. Instrum.* **2002**, *73*, 3469.

(25) *Handbook of the Optical Constants of Solids*; Palik, E. D., Ed.; Academic: Toronto, 1985.

(26) Greenler, R. G. *J. Chem. Phys.* **1966**, *44*, 310.

(27) Toon, O. B.; Tabazadeh, A.; Browell, E.. V.; Jordan, J. *J. Geophys. Res.* **2000**, *105*, 20589.

(28) Reichardt, J.; Reichardt, S.; Yang, P.; McGee, T. J. *J. Geophys. Res.* **2002**, *107*, 8282.

(29) Voigt, C.; Shreiner, J.; Kohlmann, A.; Zink P.; Mauersberger, K.; Larsen, N.; Deshler, T.; Kröger, C.; Rosen, J.; Adriani, A.; Cairo, F.; Di Donfrancesco, G.; Viterbini, M.; Ovarlez, J.; Ovarlez, H.; David, C.; Dörnbrack, A. *Science* **2000**, *290*, 1756.